Analyses on Though-Bolts Type Wooden Beam-Column Joints Subjected to Rotational Moment

Kohei Komatsu

Abstract

This paper introduces an examples of analyses on the elasto-plastic behavior of so-called “through-bolts type” wooden beam-column steel joints which are widely used in modern wooden residential houses recent in Japan. The analyses were done on two parts, one of which was “glulam column-steel gusset joint” where column and gusset are connected by using “though bolts” and the other part was “steel gusset-glulam beam joint” where gusset and beam are connected by using drift pins. By the theoretical analyses, initial stiffness, yielding moment and second stiffness were derived so as to include various parameters in a closed form. Full scale experiments were also carried out using three replications on two different types of test specimens. Comparisons between theoretical predictions and experimental observations showed good agreements.

Key words: mechanical model, embedment, drift pin (DP), rotational stiffness, yielding moment.

Introduction

In recent modern wooden post and beam style residential houses, many of super-structures are tended to be composed of glued laminated timber (denoted as “glulam” hereafter) columns and beams with using prefabricated engineered steel joints as shown in Figure.1.

In such modern connection systems, their initial stiffness, yielding strength, ductility and ultimate strength are usually ensured by both sufficient experimental and theoretical researches done by collaborating with university’s researchers like this article case. In this paper, an examples of analyses on the behavior of so-called “through-bolts type wooden beam-column joints” subjected to rotational moment is introduced with some full-scale experimental results.

Mechanical Model of Beam-Column Joint

Figure 2 shows a beam-column joint subjected to a rotational moment. This joint constitutes from two parts, one of which is “glulam column-steel gusset joint” where column and gusset are connected by using “though bolts” and the other part is “steel gusset-glulam beam joint” where gusset and beam are connected by using drift pins. Therefore analysis should be done separately in each part, then these independent rotational deformations will be combined to obtain an apparent one rotational spring.

Rotational Stiffness of Column-side Joint

Figure 3 shows deformed configuration and reaction forces on column-steel connection subjected to a clock-wise rotation moment $+M$

The relationship between tensile force T_j and elongation e_{Bj} acting on the j-th bolt which connects between the column and steel connector.

$$e_{Bj} = \frac{T_j}{K_{Bj}} \qquad (j=2、3) \qquad \ldots(1)$$

where,

$K_{Bj} = \dfrac{E_{Bj} A_{Bj}}{l_{Bj}}$: axial stiffness of j-th bolt (N/mm)

E_{Bj} : Young’s modulus of j-th bolt (N/mm^2)

A_{Bj} : effective cross sectional area of j-th bolt

$$= \frac{{d_j}^2 \pi}{4} \text{ (mm}^2\text{)} \qquad \ldots(2)$$

d_j : effective diameter of j-th bolt (mm)

l_B : effective elongation length of j-th bolt (mm)

g_B : distance from bottom of beam to j-th bolt (mm)

Figure 1. Typical construction site of modern wooden post and beam style residential house.

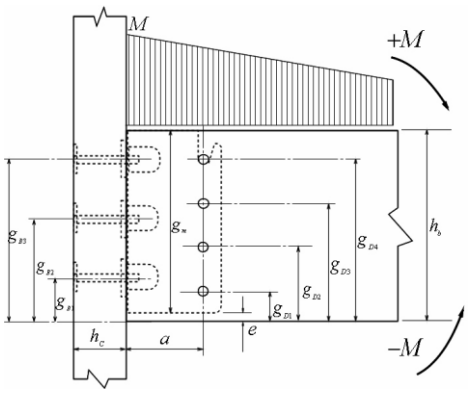

Figure 2. A beam-column joint subjected to a rotational moment.

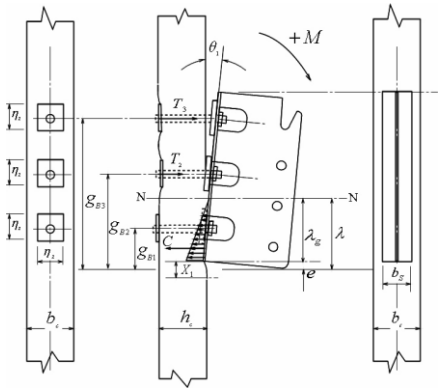

Figure 3. Deformed configuration and reaction forces on column-steel connection subjected to a rotational moment *+M*.

The quantity of embedment of bearing plate into back side of column is to be evaluated based on the assumption proposed by Inayama (1991). For the coefficient for surface deformation function a_C which governs the effect of extended free surface of the embedment of timber perpendicular to the grain, new proposal, in which various coefficients were re-defined in accordance with corresponding boundary conditions, were quoted from the research result published recently by Kitamori *et al*. (2009). Hence, equations (3) to (7) were obtained for the embedment of bearing plate occurring at the back surface of column;

$$e_{Zj} = \frac{T_j}{K_{Zj}} \quad \ldots(3)$$

where,

$$K_{Zj} = \frac{{\eta_Z}^2 C_{xc} C_{yc} E_{90}}{h_c} \quad \ldots(4)$$

$$C_{xc} = 1 + \frac{2}{a_C \eta_Z}\left(1 - e^{-\frac{a_C x_1}{h_c}}\right) \quad \ldots(5)$$

$$C_{yc} = 1 + \frac{2}{a_C n \eta_Z}\left\{1 - e^{-a_C n(b_c - \eta_Z)}\right\} \quad \ldots(6)$$

The coefficient for surface deformation function a_C is;

$$a_C = \frac{4.5}{h_c} \quad \ldots(7)$$

Further more,

$E_{90} = E_0 / 25$ (N/mm²): Modulus of elasticity perpendicular to the grain which is quoted from the design standard for timber construction (AIJ 2006)

η_Z : length of one edge of square bearing plate(mm)

b_c : width of column (mm)

n : ratio for the perpendicular to the grain against parallel to the grain. This vale is assigned for species group, foe example, *n*=7 for J1, *n*=6 for J2 and *n*=5 for J3 group, respectively.

Resultant compression force C, which is brought by embedment of the vertical steel plate of connector into the side surface of column, by applying another assumption for triangular embedment proposed by Inayama (1999) and for a_T by Kitamori *et al*. (2009) as shown in equation (8).

$$C = \frac{(\lambda - e)^2 b_S C_{xT} C_{yT} E_{90}}{2h_c}\theta_1 \quad \ldots(8)$$

where,

$$C_{xT} = 1 + \frac{2}{a_T(\lambda - e)}\left(1 - e^{-\frac{a_T x_1}{h_c}}\right) \quad \ldots(9)$$

$$C_{yT} = 1 + \frac{2}{a_T n b_S}\left(1 - e^{-\frac{a_T n(b_c - b_S)}{2h_c}}\right) \quad \ldots(10)$$

$$a_T = \frac{4.5}{h_c} \quad \text{(Kitamori et al 2009)} \quad \ldots(11)$$

and,

b_S : contact width of vertical steel plate (mm)

X_1 : effective length of extended free surface. In case of Figure.2, X_1 was assumed as infinite.

Total deformation e_{Tj} of j-th bolt subjected to the tensile force T_j can be estimated as the summation of the elongation of bolt e_{Bj} and embedment of bearing plate into back surface of column e_{Zj} ;

$$e_{Tj} = e_{Bj} + e_{Zj} \quad \ldots(12)$$

Substituting equations (1) and (2) into (12)

$$e_{Tj} = \frac{T_J}{K_{Bj}} + \frac{T_j}{K_{Zj}} = \left(\frac{1}{K_{Bj}} + \frac{1}{K_{Zj}}\right) T_j \quad \ldots(13)$$

It might be possible to assume the following approximate geographical relationship on the total deformation e_{Tj} and rotation angle θ_1 between column and steel plate.

$$e_{Tj} \cong (g_{Bj} - \lambda)\theta_1 \quad \ldots(14)$$

Substituting equation (14) into equation (13),

$$\left(\frac{K_{Zj} + K_{Bj}}{K_{Bj} K_{Zj}}\right) T_j = (g_{Bj} - \lambda)\theta_1$$

$$\rightarrow T_j = \left(\frac{K_{Bj} K_{Zj}}{K_{Zj} + K_{Bj}}\right)(g_{Bj} - \lambda)\theta_1 \quad \ldots(15)$$

Equilibrium of forces is,

$$T_2 + T_3 = C \quad \ldots(16)$$

Substituting equation (16) into equations (8) and (15),

$$\left(\frac{K_{B2} K_{Z2}}{K_{Z2} + K_{B2}}\right)(g_{B2} - \lambda)\theta_1 + \left(\frac{K_{B3} K_{Z3}}{K_{Z3} + K_{B3}}\right)(g_{B3} - \lambda)\theta_1 = \frac{(\lambda - e)^2 b_S C_{xT} C_{yT} E_{90}}{2h_c}\theta_1 \quad \ldots(17)$$

As X_1 in C_{xT} can be infinite by considering content of equations (9) and (10),

$$C_{xT} \cong 1 + \frac{2}{a_T(\lambda - e)} \quad \ldots(18)$$

Also the y-directional effect of extend length involved in the assumption of Inayama (1999) might not be expected because the deference between width of column b_c and contact width of steel plate b_S is so small,

$$C_{yT} \cong 1 \quad \ldots(19)$$

Taking account the above mentioned approximate conditions into equation (17), we get following second order formula of λ without respect to θ_1 ,

$$\left(\frac{K_{B2} K_{Z2}}{K_{Z2} + K_{B2}}\right)(g_{B2} - \lambda) + \left(\frac{K_{B3} K_{Z3}}{K_{Z3} + K_{B3}}\right)(g_{B3} - \lambda) = \frac{(\lambda - e)^2 b_S \left\{1 + \frac{2}{a_T(\lambda - e)}\right\} E_{90}}{2h_c}$$

$$\rightarrow \lambda^2 - 2\left\{e - \left(\frac{1}{a_T}\right) - \left(\frac{h_c}{b_s E_{90}}\right)\sum_{j=2}^{3}\left(\frac{K_{Bj} K_{Zj}}{K_{Zj} + K_{Bj}}\right)\right\}\lambda - \left\{\left(\frac{2e}{a_T} + e^2\right) + \left(\frac{2h_c}{b_s E_{90}}\right)\sum_{j=2}^{3}\left(\frac{K_{Bj} K_{Zj}}{K_{Zj} + K_{Bj}}\right) g_{Bi}\right\} = 0 \quad \ldots(20)$$

Hence the location of the neutral axis is obtained as equation (21).

$$\lambda = \pm\sqrt{\alpha^2 + \beta} + \alpha \quad \ldots(21)$$

where

$$\alpha = \left\{e - \left(\frac{1}{a_T}\right) - \left(\frac{h_c}{b_s E_{90}}\right)\sum_{j=2}^{3}\left(\frac{K_{Bj} K_{Zj}}{K_{Zj} + K_{Bj}}\right)\right\}$$

$$\beta = \left\{\left(\frac{2e}{a_T} + e^2\right) + \left(\frac{2h_c}{b_s E_{90}}\right)\sum_{j=2}^{3}\left(\frac{K_{Bj} K_{Zj}}{K_{Zj} + K_{Bj}}\right) g_{Bi}\right\} \quad \ldots(22)$$

From the equilibrium among forces and external moment at interface between column and steel plate, external moment M can be expressed by equation (23).

$$M = (g_{B2} - \lambda)T_2 + (g_{B3} - \lambda)T_3 + \frac{2}{3}(\lambda - e)C = R_{Jc}\theta_1 \quad \ldots(23)$$

R_{Jc} is defined as the rotational stiffness between column and steel plate as,

$$R_{Jc} = \sum_{j=2}^{3}(g_{Bj} - \lambda)^2\left(\frac{K_{Bj}K_{Zj}}{K_{Zj} + K_{Bj}}\right) + \frac{(\lambda - e)^3 b_S C_{xT} C_{yT} E_{90}}{3h_c} \quad \ldots(24)$$

Derivation of Rotational Stiffness between Steel Plate and Drift-pin (DP) Joint at Beam End

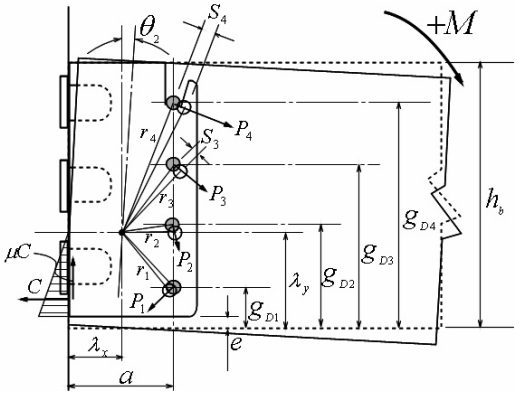

Figure 4. Schematic diagram for deformation and forces acting on beam side joint.

For the next step, the rotational stiffness between steel plate and DP joint at beam end will be derived. Figure 4 indicates a schematic diagram for deformation and forces acting on beam side joint.

Denoting location of neutral axis as λ_x and λ_y for x, y direction respectively, relationship between slip S_j of j-th DP and relative rotation angle θ_2, between steel plate and glulam beam, is approximately estimated as equation (25).

$$S_j \cong r_j\theta_2 = \sqrt{(a - \lambda_x)^2 + (g_{Dj} - \lambda_y)^2}\,\theta_2 \quad \ldots(25)$$

Relationship between force P_j and slip S_j of j-th DP is expressed as equation (26).

$$P_j = K_{\phi j} \cdot S_j \quad \ldots(26)$$

Here, $K_{\phi j}$ is ϕ_j-directional slip modulus of j-th DP which might be estimated by using so-called Hankinson's equation (27) (AIJ 2009).

$$K_{\phi j} = \frac{K_0 \cdot K_{90}}{\left(K_0 \sin^2\phi_j + K_{90}\cos^2\phi_j\right)} \quad \ldots(27)$$

$$\phi_j = \frac{\pi}{2} - \tan^{-1}\left(\frac{g_{Dj} - \lambda_y}{a - \lambda_x}\right) \quad \ldots(28)$$

Slip moduli K_0, K_{90} in equation (27) can be derived as equations (29) and (30) by employing "the theory of beam on the elastic foundation" by setting boundary conditions as shown in Figure 5 (AIJ 2009).

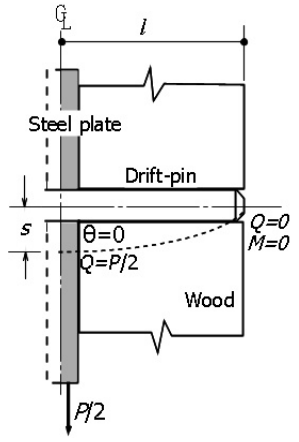

Figure 5. Boundary conditions for steel insert type DP-joint (AIJ 2009)

$$K_{0j} = 4\Phi_0\lambda_0{}^3(EI)_s \tanh\lambda_0 l$$
$$\lambda_0 = \sqrt[4]{\frac{k_{w0}d}{4(EI)_s}},\ \Phi_0 = 2\left(\frac{1 - r_0 q_0}{1 + r_0{}^2}\right)$$
$$r_0 = \frac{\cos\lambda_0 l}{\cosh\lambda_0 l},\ q_0 = \frac{\sin\lambda_0 l}{\sinh\lambda_0 l}$$

Slip modulus for insert-type DP-joint parallel to the grain direction …(29)

$$K_{90j} = 4\Phi_{90}\lambda_{90}{}^3(EI)_s \tanh\lambda_{90} l$$
$$\lambda_{90} = \sqrt[4]{\frac{k_{w90}d}{4(EI)_s}},\ \Phi_{90} = 2\left(\frac{1 - r_{90} q_{90}}{1 + r_{90}{}^2}\right)$$
$$r_{90} = \frac{\cos\lambda_{90} l}{\cosh\lambda_{90} l},\ q_{90} = \frac{\sin\lambda_{90} l}{\sinh\lambda_{90} l}$$

Slip modulus for insert-type DP-joint perpendicular to the grain direction …(30)

here,

k_{w0} : embedment coefficient parallel to the grain direction by circular steel dowel of diameter d and to be estimated by equation (31) (AIJ 2006).

k_{w90} : embedment coefficient perpendicular to the grain direction by circular steel dowel of diameter d and to be estimated by equation (32) (AIJ 2006).

$$k_{w0} = \frac{E_0}{(31.6 + 10.9d)} \quad \text{(N/mm}^3\text{)} \qquad \ldots(31)$$

$$k_{w90} = k_{w0} / 3.4 \quad \text{(N/mm}^3\text{)} \qquad \ldots(32)$$

E_0 : Modulus of elasticity of timber parallel to the grain(N/mm^2)

$(EI)_s$: Flexural rigidity of DP(Nmm^2)

d : diameter of DP(mm)

l_e : effective DP length (mm), and this value has a relationship with l and t in Figure 4, as follows;

$$l_e = 2l + t \qquad \ldots(33)$$

Substituting equations (25) and (27) into equation (26), we obtain,

$$P_j = K_{\phi j} \cdot S_j = K_{\phi j} \cdot \sqrt{(a - \lambda_x)^2 + (g_{Dj} - \lambda_y)^2}\,\theta_2 \qquad \ldots(34)$$

$K_{\phi j}$ in equation (34) is a function of λ_x and λ_y, however, as the derivation process becomes quite complicated unless they are considered as constant, in this stage they were considered as constant and after λ_x, λ_y are tentatively determined, all variables should be re-estimated by employing several times iterations in Excel-sheet until converged values are obtained.

Figure 6 shows definition of the force P_j acting on j-th DP and its x, y components P_{j-x} ,and P_{j-y} .

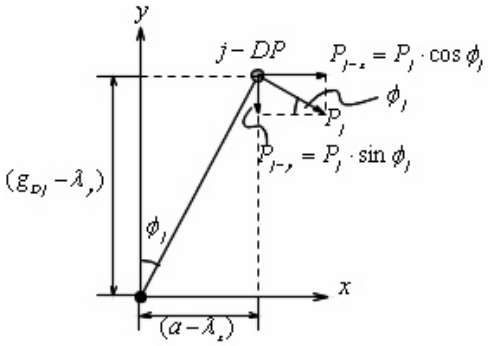

Figure 6. Definition of the force P_j acting on j-th DP and its x, y components P_{j-x} , and P_{j-y} .

From geometrical relationships we get,

$$\sin\phi_j = \frac{(a - \lambda_x)}{\sqrt{(a - \lambda_x)^2 + (g_{Dj} - \lambda_y)^2}}$$

$$\cos\phi_j = \frac{(g_{Dj} - \lambda_y)}{\sqrt{(a - \lambda_x)^2 + (g_{Dj} - \lambda_y)^2}} \qquad \ldots(35)$$

Combining equations (34) and (35), we obtained equations (36) and (37) for x, y component of P_j

$$P_{j-x} = P_j \cdot \cos\phi_j = (g_{Dj} - \lambda_y) \cdot K_{\phi j}\theta_2 \qquad \ldots(36)$$

$$P_{j-y} = P_j \cdot \sin\phi_j = (a - \lambda_x) \cdot K_{\phi j} \cdot \theta_2 \qquad \ldots(37)$$

While, as the end grain surface of beam is subjected to a "triangularly distributing compression force" (Inayama 1991) by the action of steel vertical plate, the resultant compression force will be calculated as,

$$C = b_{se} \int_0^{\lambda_y - e} k_o y \theta_2 dy = \frac{b_{se} k_0 (\lambda_y - e)^2}{2} \theta_2 \qquad \ldots(38)$$

where,

k_0 :embedment coefficient of wood subjected to compression stress parallel to the grain (N/mm^3). This quantity was recently re-defined by using the assumption of Inayama (2009), and in this article k_0 was determined as equation (39) by considering corresponding boundary condition.

$$k_0 = \frac{5E_0\left(0.08 + \frac{1}{b_{se}}\right)}{(70.6 - 0.3b_{se})} \qquad \ldots(39)$$

here,

b_{se} : effective contact width defined as vertical steel plate width minus thickness of center plate (mm)

Equilibrium of forces for x-direction is expressed as equation (41).

$$P_{1-x} + C = P_{2-x} + P_{3-x} + P_{4-x} \qquad \ldots(41)$$

Substituting equations (36) and (38) into equation (41), we get equation (42).

$$(g_{D1} - \lambda_y) \cdot K_{\phi 1} \cdot \theta_2 + \frac{b_{se} k_0 (\lambda_y - e)^2}{2} \theta_2 = \sum_{j=2}^{4} (g_{Dj} - \lambda_y) \cdot K_{\phi j} \cdot \theta_2$$

$$\rightarrow {\lambda_y}^2 - 2\left(\frac{1}{b_{se}k_0}K_{\phi 1} - \frac{1}{b_{se}k_0}\sum_{j=2}^{4}K_{\phi j} + e\right)\lambda_y + \frac{2}{b_{se}k_0}\left(g_{D1}K_{\phi 1} - \sum_{j=2}^{4}g_{Dj}K_{\phi j}\right) + e^2 = 0 \quad \ldots(42)$$

Equation (42) gives the roots for λ_y as equation (43).

$$\lambda_y = \alpha_2 \pm \sqrt{{\alpha_2}^2 - \beta_2} \quad \ldots(43)$$

where,

$$\left.\begin{aligned}\alpha_2 &= \left(\frac{1}{b_{se}k_0}K_{\phi 1} - \frac{1}{b_{se}k_0}\sum_{j=2}^{4}K_{\phi j} + e\right)\\ \beta_2 &= \frac{2}{b_{se}k_0}\left(g_{D1}K_{\phi 1} - \sum_{j=2}^{4}g_{Dj}K_{\phi j}\right) + e^2\end{aligned}\right\} \quad \ldots(44)$$

While, equilibrium of forces for y-direction is,

$$\mu C = \sum_{1}^{4}P_{j-y} \quad \ldots(45)$$

where,

μ : friction coefficient between end grain of glulam and steel plate, and this was assumed as 0.4.

Substituting (37), (38) into (45), we get,

$$\frac{b_{se}k_0\mu(\lambda_y - e)^2}{2} - \sum_{1}^{4}(a - \lambda_x)K_{\phi j} = 0$$

$$\rightarrow \lambda_x = a - \frac{1}{2}\left\{\frac{\mu \cdot b_{se}k_0(\lambda_y - e)^2}{\sum_{j=2}^{4}K_{\phi j}}\right\} \quad \ldots(46)$$

In actual calculation process, value of λ_x and λ_y were determined by repeating several times of calculations from equations (27) till (46) until converged value was obtained.

Rotational moment M_a around the neutral axis is,

$$M_a = \sum_{1}^{4}\sqrt{(g_{Dj} - \lambda_y)^2 + (a - \lambda_x)^2}P_j + \frac{2}{3}(\lambda_y - e)C + \mu C\lambda_x = R_{Jb}\theta_2 \quad \ldots(47)$$

where,

$$R_{Jb} = \sum_{1}^{4}\left\{(g_{Dj} - \lambda_y)^2 + (a - \lambda_x)^2\right\}K_{\phi j} + \left\{\frac{2(\lambda_y - e)}{3} + \mu\lambda_x\right\}\frac{b_{se}k_0(\lambda_y - e)^2}{2} \quad \ldots(48)$$

(rotational rigidity between steel plate and beam end subjected to $+M$)

Combined Single Spring for Apparent Beam-column Joint

As the beam-column joint is constituted from two sub-springs mentioned above, it might be easier for practical engineer to merge these two sub-springs into a single apparent spring. Let define relationships of rotation angle and moment for each sub-spring as equations (49) and (50),(51).

[Rotational spring between column-steel plate]

$$\theta_1 = \frac{M}{R_{Jc}} \quad \ldots(49)$$

[Rotational spring between steel plate and beam end]

$$\theta_2 = \frac{M_a}{R_{Jb}} \quad \ldots(50)$$

$$M_a = \omega \cdot M \quad \ldots(51)$$

where, $\omega \leq 1$ and ω will be confirmed when actual moment distribution is given. For example, in the case of T-joint specimen shown in the later section for the experimental set-up, equation (51) will hold good as $M_a = \{(L - \lambda_x)/L\}M$, thus ω should be obtained as,

$$\omega = \frac{L - \lambda_x}{L} \quad \ldots(52)$$

A combined rotation angle which is constituted from two sub-springs is estimated as equation (53).

$$\theta = \theta_1 + \theta_2 = \frac{M}{R_{Jc}} + \frac{M_a}{R_{Jb}} = \left(\frac{1}{R_{Jc}} + \frac{\omega}{R_{Jb}}\right)M = \left(\frac{R_{Jb} + \omega R_{Jc}}{R_{Jc} \cdot R_{Jb}}\right)M \quad \ldots(53)$$

Therefore, moment-rotation relationship for the apparent beam-column joint is expressed as,

$$M = R_{J-bc}\theta \quad \ldots(54)$$

where, a combined rotational stiffness of the apparent beam-column joint is given as equation (55).

$$R_{J-bc}=\left(\frac{R_{Jc}\cdot R_{Jb}}{R_{Jb}+\omega R_{Jc}}\right)\ \text{(Nmm/rad)} \qquad \ldots(55)$$

Yielding Moment of Beam-Column Joint

Here, two possible yielding criteria are assumed.

[*First yielding criterion*]

The first one is a yielding moment which might be caused by embedment of vertical steel plate onto side surface of column. According to the assumption by Inayama (1991), yielding rotation angle for triangular embedment is given as equation (56).

$$\theta_{1y}=\frac{F_m h_c}{\lambda_g E_{90}\sqrt{C_{xT}C_{yT}C_{xTm}C_{yTm}}} \qquad \ldots(56)$$

where,

F_m : partial compression strength perpendicular to the grain that will be appropriate if 80% of the basic material strength value should be used (Kitamori et al. 2009). Parameters in equation (56) are as follows.

$$C_{xT}=1+\frac{2}{a_T\lambda_g}\left(1-e^{-\frac{a_T x_1}{h_c}}\right),$$

$$C_{yT}=1+\frac{2}{a_T n b_S}\left(1-e^{-\frac{a_T n(b_c-b_S)}{2h_c}}\right),$$

$$C_{xTm}=1+\frac{2}{a_T\lambda_g},\ C_{yTm}=1+\frac{2}{a_T n b_S}$$

Yielding moment at column side can be given as,

$$M_{yT}=R_{Jc}\cdot\theta_{1y} \qquad \ldots(57)$$

Apparent yielding rotation angle at beam-column joint is thus given by the equation (58).

$$\theta_Y=\frac{M_{yT}}{R_{J-cb}} \qquad \ldots(58)$$

[*Second yielding criterion*]

The second one is a yielding which might be caused by embedment of bolt bearing plate onto side surface of column. According to the assumption by Inayama (1991), yielding deformation due to partial compression force by bolt bearing plate is given as,

$$e_Z=\frac{h_c F_m}{E_{90}\sqrt{C_{xC}C_{yC}C_{xCm}C_{yCm}}} \qquad \ldots(59)$$

At this stress level, it might be possible to assume that the tensile force T_3, which is supposed as the maximum axial force among all bolts, could be estimated as a product of F_m times bearing area ($\eta_Z \times \eta_Z$), thus, elongation of bolt at the yielding level might be calculated as,

$$e_B=\frac{T_{3y}}{K_{B3}}=\frac{F_m{\eta_Z}^2}{K_{B3}} \qquad \ldots(60)$$

Therefore, total elongation of the corresponding bolt can be estimated as,

$$e_y=e_Z+e_B=\frac{h_c F_m}{E_{90}\sqrt{C_{xC}C_{yC}C_{xCm}C_{yCm}}}+\frac{F_m{\eta_Z}^2}{K_{B3}} \qquad \ldots(61)$$

Rotation angle at column side sub-spring is,

$$\theta_{1y}=\frac{e_y}{(g_{B3}-\lambda)}$$

$$=\frac{F_m}{(g_{B3}-\lambda)}\left[\frac{h_c}{E_{90}\sqrt{C_{xC}C_{yC}C_{xCm}C_{yCm}}}+\frac{{\eta_Z}^2}{K_{B3}}\right] \qquad \ldots(62)$$

Corresponding moment acting at column side sub-spring is,

$$M_{yZ}=R_{Jc}\cdot\theta_{1y} \qquad \ldots(63)$$

Therefore, apparent yielding rotation angle for beam-column joint is,

$$\theta_Y=\frac{M_{yZ}}{R_{J-cb}} \qquad \ldots(64)$$

Consequently, yielding of an apparent beam-column joint will be determined from the smaller value of both yielding moments as defined in equation (65),

$$M_Y=\mathrm{Min}\{M_{yT}\ 、\ M_{yZ}\} \qquad \ldots(65)$$

Post-Yielding Rotational Stiffness of Beam-Column Joint

Post-yielding behaviour might be calculated using the same equations as those in elastic case from equation (1) to (55) by using post-yielding modulus of elasticity of column E_{90} as 1/8 of that in elastic case in accordance with the suggestion from Inayama (AIJ 2009). Comparisons between experimental observations and theoretical predictions for the post-yielding behaviour will be done using equation (66) under the assumption that specimen will not fail at least until the rotation angle θ_u which was observed maximum rotation angle.

$$M_u=R_{J-cb2}(\theta_u-\theta_Y)+M_Y \qquad \ldots(66)$$

where,

R_{J-cb2} : beam-column combined rotational stiffness calculated by using $E_{90-2}=E_{90-1}/8$ (Nmm/rad)

θ_u : observed ultimate rotation angle (rad)

θ_Y : predicted rotation angle at yielding (rad)

M_Y : predicted yielding moment by equation (65) (Nmm)

Experiments

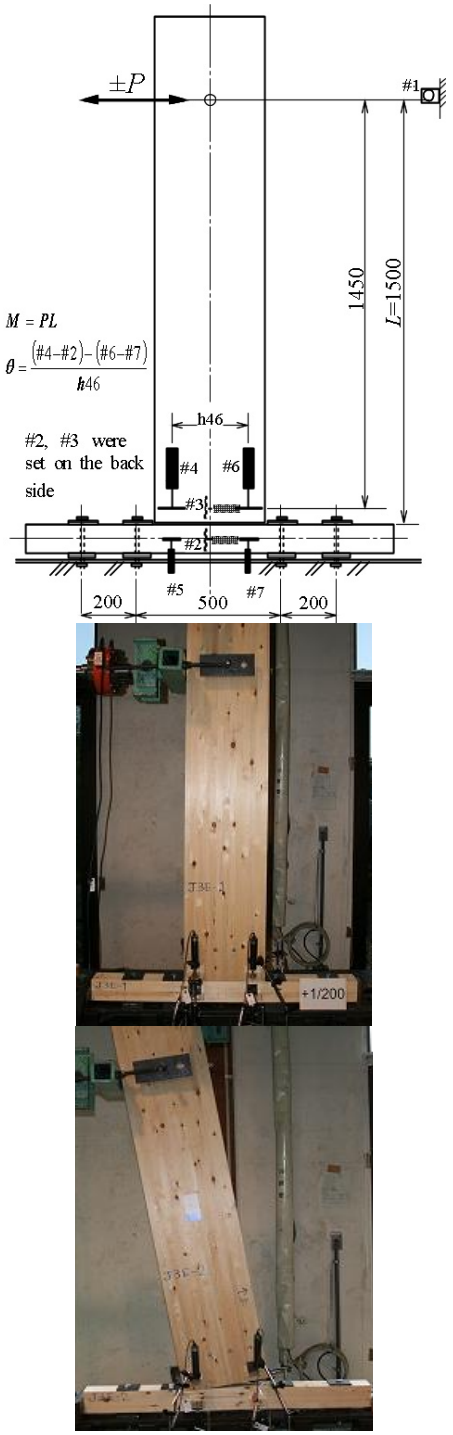

Figure 7. Test set-up and deformed situation of T-shaped beam-column joint subjected to a lateral force.

The aim of this article is to show how generalized mechanical model of beam-column joint, composed of steel gusset plate with which column is connected by through bolts, as well as beam is connected by drift pins, could be derived in details. Therefore description on the experimental procedures or/and experimental results would be shown as less as possible. Figure 7 shows a feature of experimental set-up subjected to static push-pull lateral load. Table 1 summarizes material constant of test specimen and some representative geometries of members by which numerical calculations were done.

Table 1. Material constants of test specimen and some representative geometry of members.

d_j	diameter of bolt (mm)	12
l_{Bj}	effective length of bolt (mm)	105
E_B	young's modulus of bolt (N/mm^2)	206010
$E_{0\text{-}1}$	young's modulus of column parallel to the grain before yield (N/mm^2)	9320
$E_{90\text{-}1}$	young's modulus of column perpendicular to the grain before yield (N/mm^2)	373
E_{w0}	young's modulus of beam parallel to the grain (N/mm^2)	10301
h_c	depth of column member (mm)	105
h_b	depth of beam member (mm)	390
b_b	width of beam member (mm)	105
d	diameter of drift pin (mm)	20
e	distance from bottom of beam to bottom of steel gusset (mm)	22
b_c	width of column member (mm)	105
b_s	width of contact steel vertical plate (mm)	77
t	thickness of steel gusset plate (mm)	6
g_{B1}	lower bolt location from bottom of beam (mm)	92
$g_{Bj+1} - g_{Bj}$	adjacent bolt distance (mm)	120
g_m	height of steel gusset plate (mm)	368
g_{D1}	lower drift pin location from bottom of beam (mm)	62
$g_{Dj+1} - g_{Dj}$	adjacent drift pin distance (mm)	90
a	distance of drift pin from end grain (mm)	156
l_e	effective drift pin length (mm)	99

Results and Discussion

Figures 8a), b) and c) show comparisons between observed moment-rotation angle relationships and predicted bi-linear moment-rotation angle relationships for plus moment region. For the initial stiffness and yielding moment, coincidence between theoretical predictions and experimental observations seems to be good. While for the post-yielding behavious, there are slight discrepancies between theoretical predictions and experimental observations. For the stage of post-yielding, as no rigorous theoretical considerations were given except simply obeying the assumption proposed by Inayama (1991) telling that the young's modulus perpendicular to the grain of timber tended to show value of about 1/8 times of that shown in elastic range, the predictions

seemed to become rough in the actual post-yielding range.

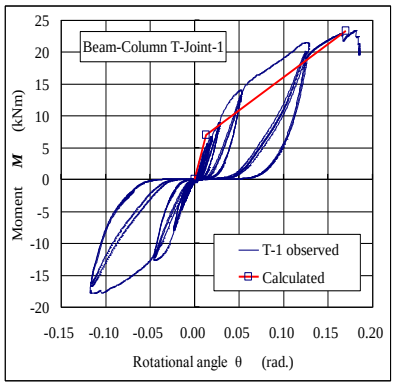

a) T-1 specimen

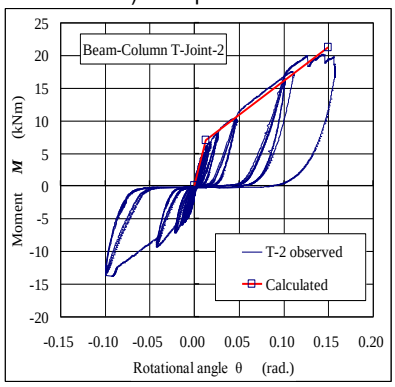

b) T-2 specimen

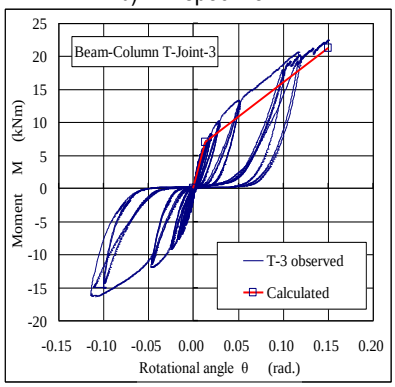

c) T-3 specimen

Figure 8. Comparisons between observed moment-rotation relationships and predicted bi-linear relationship.

Therefore, by considering another equilibrium condition where some resultant forces should be in plastic or highly low stiffness range, more realistic non-linear behavious might be able to obtain. In addition to this imperfect model, the author did not measure any material constants directly by using the same materials used in the experiments. That might be another cause for a bit discrepancy between theory and observation. From practical point of view, however, agreement between theory and experiment shown in Figure 7 might be acceptable. In consequent, further analyses will be necessary based on the level of demands how precisely the post-yielding behaviors should be predicted.

Acknowledgements

Part of this study was supported by a budget given by the Japan Society for Promoting Science (JSPS). Agreement to submitting this content to this journal was given by a company. The author would like to express his sincere appreciations for both JSPS and a company.

References

AIJ (Architectural Institute of Japan; edited). 2006. Standard for Structural Design of Timber Structures, Maruzen, p.164. 4th edition. (in Japanese).

AIJ (Architectural Institute of Japan; edited). 2009. Drift-pined Joint with Steel Insert Plate, Design Manual for Engineered Joints in Timber Construction, 195-206, (in Japanese).

Inayama, M. 1991. Embedment Theory and Its Application, Ph.D Thesis submitted to Tokyo University. (in Japanese).

Inayama, M. 2009. Proposal of Embedment Stiffness Equation for Wooden Interlocking Joints Based on the Embedment Theory. Summary of 59th Annual Meeting of Japan Wood Research Society, PH007, CR-ROM. (in Japanese).

Kitamori, A.; T. Mori; Y. Kataoka; K. Komatsu. 2009. Effect of Additional Length on Partial Compression Perpendicular to the Grain of Wood. Journal of Structural and Construction Engineering, Transactions of AIJ, 74(642): 1477-1485. (in Japanese).

Kohei Komatsu

Laboratory of Structural Function

Research Institute for Sustainable Humanosphere

Kyoto University

Uji City, Kyoto Prefecture, Japan 611-0011.

E-mail: kkomatsu@rish.kyoto-u.ac.jp